7
Scintillation counters

One of the most commonly used particle detectors is the scintillation counter. A fraction of the energy lost by a charged particle can excite atoms in the scintillating medium. A small percentage of the energy released in the subsequent deexcitation can produce visible light. The technique has been used since the earliest investigations of radioactivity, when, for instance, Rutherford used scintillating ZnS crystals in his alpha particle scattering experiments.

In modern detectors light produced in the scintillator is propagated through light guides and directed onto the face of a photomultiplier tube. Photoelectrons emitted from the cathode of the tube are amplified to give a fast electronic pulse, which can be used for triggering or timing applications.

7.1 The scintillation process

We define a scintillator to be any material that produces a pulse of light shortly after the passage of a particle. The phenomenon is closely related to fluorescence, which is usually defined to be the production of a light pulse shortly following the absorption of a light quantum [1, 2]. "Shortly" here refers to time intervals on the order of 10 ns or less. Phosphorescence is a third phenomenon involving light emission, but in this case the molecules are left in a meta-stable state, and the emission may occur much later than the initiating event.

Both inorganic and organic scintillators have been discovered. The scintillation process is different for the two groups. Inorganic crystals are usually grown with a small admixture of impurity centers. The most important example is NaI doped with thallium. The positive ions and electrons created by the incoming particle diffuse through the lattice and

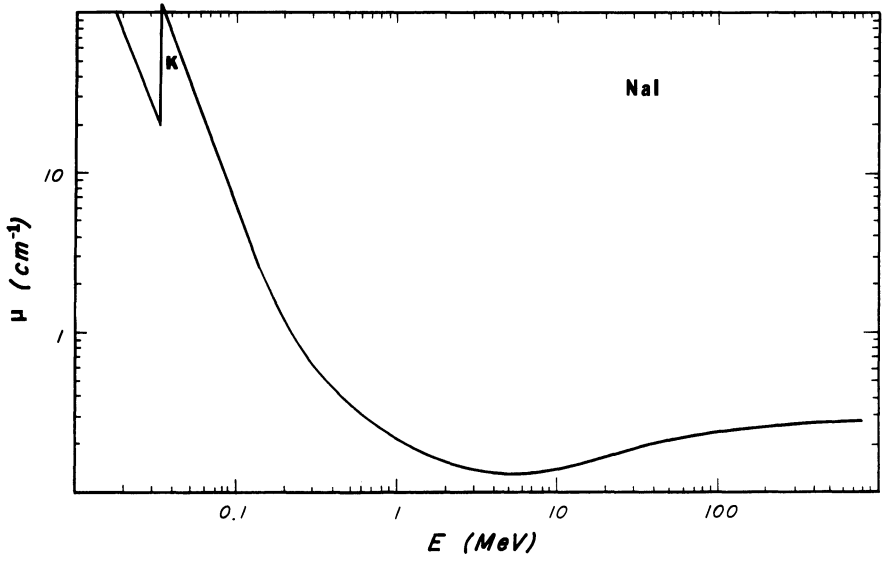
Downloaded from https://www.cambridge.org/core. UNIVERSIDAD AUTONOMA METROPOLITANA, on 14 Nov 2026 at 11:01:54, subject to the Cambridge Core terms of use, available at https://www.cambridge.org/core/terms. https://doi.org/10.1017/9781009290098.008

are captured by the impurity centers [1, 3, 4]. Recombination produces an excited center, which emits light upon its return to the ground state. The light output is larger than that of the organic materials, but the electron migration through the crystal lattice results in a pulse ($\sim 1.5\ \mu s$) of much longer duration. The light output per unit absorbed energy of inorganic scintillators has a significant temperature dependence.

NaI crystals are hygroscopic, so the counters must be protected from water vapor. The emission spectrum of a NaI(Tl) crystal is significant over the range 340–490 nm. NaI scintillators are widely used as photon detectors because of their relatively high density and atomic number. Figure 7.1 shows the photon linear attenuation coefficient for NaI. Some properties of NaI, CsI, and bismuth germanate (BGO) are shown in Table 7.1. BGO is also finding acceptance for high resolution photon detection [5]. It has a radiation length of 1.12 cm, which is shorter than NaI, and it is nonhygroscopic. On the other hand, it is more expensive and has a smaller light output.

The organic scintillators can be further subdivided into organic crystals, liquid scintillators, and plastic scintillators. The advantages of the organic materials include transparency to their own radiation, short

Figure 7.1 Linear attenuation coefficient of NaI. (K) K absorption edge. (Data taken from J. Hubbell, National Bureau of Standards report NSRDS-NBS 29, 1969.)



Downloaded from https://www.cambridge.org/core. UNIVERSIDAD AUTONOMA METROPOLITANA, on 14 Nov 2026 at 11:01:54, subject to the Cambridge Core terms of use, available at https://www.cambridge.org/core/terms. https://doi.org/10.1017/9781009290098.008

decay times, emission spectra well matched to photomultipliers, and easy adaptibility.

The scintillation mechanism in organic scintillators depends strongly on the molecular structure of the medium [1, 2, 6]. After the passage of a high energy particle many of the atoms in the scintillating medium will be excited into higher energy levels. Most of the excitation energy is given up in the form of heat and lattice vibrations. However, in a scintillator some of the excitation energy is released as radiation. The scintillation efficiency is defined to be the fraction of the deposited energy that appears as radiation. The absolute efficiency of even the best scintillators is quite low, 7% for NaI and 3.5% for anthracene, the best organic material. Deexcitation without the production of radiation is sometimes referred to as quenching. The presence of even minute quantities of impurities in the organic scintillator can lead to quenching and a consequent reduction in scintillation efficiency.

Table 7.1. *Properties of scintillators*

	Relative light output	λ_{max} emission (nm)	Decay time (ns)	Density (g/cm^3)
Inorganic crystals				
NaI(Tl)	230	415	230	3.67
CsI(Tl)	250	560	900	4.51
$Bi_4Ge_3O_{12}$ (BGO)	23–86	480	300	7.13
Organic crystals				
Anthracene	100	448	22	1.25
Trans-stilbene	75	384	4.5	1.16
Naphthalene	32	330–348	76–96	1.03
p,p′-Quarterphenyl	94	437	7.5	1.20
Primary activators				
2,5-Diphenyl-oxazole (PPO)	75	360–416	5[a]	
2-Phenyl-5-(4-biphenylyl)-1,3,4-oxadiazole (PBD)	96	360–5		
4,4″-Bis(2-butyloctyloxy)-*p*-quaterphenyl (BIBUQ)	60	365,393	1.30[b]	

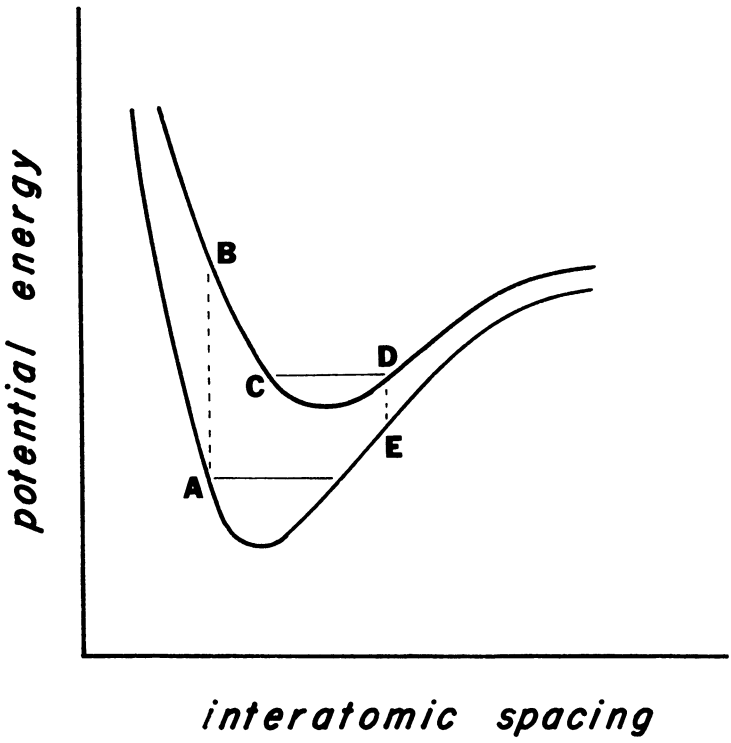
[a] 4g/l in xylene.
[b] 65 g/l in toluene.
Source: E. Schram, *Organic Scintillation Detectors,* New York: Elsevier, 1963; D. Ritson (ed.), *Techniques of High Energy Physics,* New York: Interscience, 1961; P. Pavlopoulos et al., Nuc. Instr. Meth. 197: 331, 1982; Catalog, Nuclear Enterprises Inc.; M. Moszynski and B. Bengtson, Nuc. Instr. Meth. 158: 1, 1979; B. Bengtson and M. Moszynski, Nuc. Instr. Meth. 204: 129, 1982; H. Grassmann, E. Lorenz, and H.-G. Moser, Nuc. Instr. Meth. 228: 323, 1985.

Downloaded from https://www.cambridge.org/core. UNIVERSIDAD AUTONOMA METROPOLITANA, on 14 Nov 2026 at 11:01:54, subject to the Cambridge Core terms of use, available at https://www.cambridge.org/core/terms. https://doi.org/10.1017/9781009290098.008

The light emission is governed by the electronic transitions in the molecule [2]. The electronic levels have a typical energy spacing of ~ 4 eV. The vibrational levels of the molecule ($\Delta E \sim 0.2$ eV) also play a role. Electrons in high levels typically deexcite to the lowest excited state without emission of radiation.

The emitted light is not self-absorbed because of the differing shapes of the excited and ground state energy levels as a function of interatomic spacing. We show in Fig. 7.2 the ground state and excited vibrational energy levels of a molecule. The Frank–Condon principle states that the atoms in a molecule do not change their internuclear distances during an electronic transition [2]. Thus transition ($A \rightarrow B$) from the ground state to the excited state occurs with no change in interatomic distance. The molecule finds itself out of equilibrium with its surroundings and quickly loses vibrational energy to the lattice arriving at level CD. After a short period of time the molecule will decay to some vibrational level of the ground state ($D \rightarrow E$). It then falls to the ground state by interacting with the lattice. The net result is that the molecule absorbs photons corre-

Figure 7.2 Molecular potential energy versus interatomic spacing.



Downloaded from https://www.cambridge.org/core. UNIVERSIDAD AUTONOMA METROPOLITANA, on 14 Nov 2026 at 11:01:54, subject to the Cambridge Core terms of use, available at https://www.cambridge.org/core/terms. https://doi.org/10.1017/9781009290098.008

sponding to the transition $A \rightarrow B$ and later emits lower energy photons corresponding to the transition $D \rightarrow E$.

The random excitation of scintillator material leads to an exponential time dependence for photon emission.

$$n(t) = k(1 - e^{-t/\tau}) \tag{7.1}$$

where τ is a decay time characteristic of the material. Many materials have a prompt decay when most of the light is emitted, together with a smaller, long time constant decay. The density of ionization can influence the time dependence of light emission in some media.

The amount of light produced for a given energy loss is not constant but depends on the production of quenching centers. These are activated molecules raised to excited vibrational levels. The number of produced photons roughly follows the equation [4]

$$n = \frac{n_0 dE/dx}{1 + B\, dE/dx} \tag{7.2}$$

where B and n_0 are constants and dE/dx is the ionization energy loss. The parameter B is sometimes referred to as the α to β ratio. Note that the light output saturates for large energy losses.

All organic scintillators contain a benzene ring in their structure. The organic crystals have the highest scintillation efficiency. Except for special applications, they are used as solutes in liquid and plastic scintillators. The scintillation efficiency, decay times, and wavelength of maximum emission of some organic crystals are contained in Table 7.1. The most efficient crystal is anthracene, which consists of three condensed benzene rings. Scintillation efficiencies are often quoted relative to an anthracene standard.

In a liquid scintillator an organic crystal (solute) is dissolved in a solvent. A typical concentration might be 3 g/l. Fortunately, although most interactions occur with the more numerous solvent molecules, it is possible for a large fraction of the deposited energy to be transferred to the solute. The scintillation efficiency depends on the solvent used. For example, xylene and toluene give good relative pulse heights with a PPO solute [2]. The scintillator BIBUQ dissolved in toluene has the best time resolution ($\sim$ 85 ps) of any scintillator currently available [7].

Liquid scintillator can be formulated especially for photon or neutron detection. Addition of cadmium or boron can increase the efficiency for neutron detection. Liquid scintillator is sometimes useful in large volume applications, such as the active element in large calorimeters.

Downloaded from https://www.cambridge.org/core. UNIVERSIDAD AUTONOMA METROPOLITANA, on 14 Nov 2026 at 11:01:54, subject to the Cambridge Core terms of use, available at https://www.cambridge.org/core/terms. https://doi.org/10.1017/9781009290098.008

Usually the efficiency of a scintillator can be increased by adding a secondary solute (wavelength shifter) at about 1% the concentration of the primary solute. The purpose of the wavelength shifter is to lower the self-absorption of the light emission and to produce an output that is well matched to the spectral acceptance of the photomultiplier tube. POPOP is a commonly used wavelength shifter for this purpose. Table 7.2 lists the peaks of the emission and absorption spectra of POPOP and some other common wavelength shifters. Figure 7.3 shows measurements of the absorption spectra of wavelength shifter materials. A second important use for wavelength shifters is in the light collection systems of large scintillator calorimeters [8].

Plastic scintillators are similar in composition to liquids. Polystyrene and polyvinyl toluene are commonly used base plastics, which take the place of the solvent in liquid scintillator. Most plastic scintillators have a density around 1.03 g/cm^3 and an index of refraction of 1.58. They are rugged, easy to machine, and available in large sizes. Important properties of some commercial plastic scintillators are shown in Table 7.3. The emission spectrum for the NE-102A plastic scintillator shown in Fig. 7.4 peaks around 420 nm. Recently more economical plastic scintillators using a polymethyl methacrylate base have been developed for large volume applications, such as for calorimeters [9].

Plastic scintillators have a fast response time, making them useful for triggering. However, they have rather poor spatial resolution. With aging and mishandling they may suffer minute surface cracking (crazing),

Table 7.2. *Wavelength shifters*

		λ_{abs} (nm)	λ_{emis} (nm)
POPOP	1,4-di-(2-(5-phenyl-oxazolyl))benzene	360	415–420
BBQ		382–430	500–505
BBOT	2,5-bis(5-tert-butylbenzoxazolyl(2'))thiophene	375–398	432
Dimethyl-POPOP	1,4-di-(2-(4-methyl-5-phenyl-oxazolyl))benzene	370	425–430
bis-MSB	*p*-bis(*o*-methylstyryl)benzene	367	416–425

Source: Nuclear Enterprises, Inc.; C. Woody and R. Johnson, Brookhaven National Laboratory report OG-755, 1984; V. Eckardt et al., Nuc. Instr. Meth. 155: 389, 1978; F. Klawonn et al., Nuc. Instr. Meth. 195: 483, 1982; Catalog, National Diagnostics, Somerville, NJ.

Downloaded from https://www.cambridge.org/core. UNIVERSIDAD AUTONOMA METROPOLITANA, on 14 Nov 2026 at 11:01:54, subject to the Cambridge Core terms of use, available at https://www.cambridge.org/core/terms. https://doi.org/10.1017/9781009290098.008

Figure 7.3 The absorption spectra of wavelength shifters. POPOP and BBOT: 20 mg/l in toluene, 3 mm; BBQ: in plastic, 2 mm. (Data taken from C. Woody and R. Johnson, Brookhaven report OG755, 1984.)

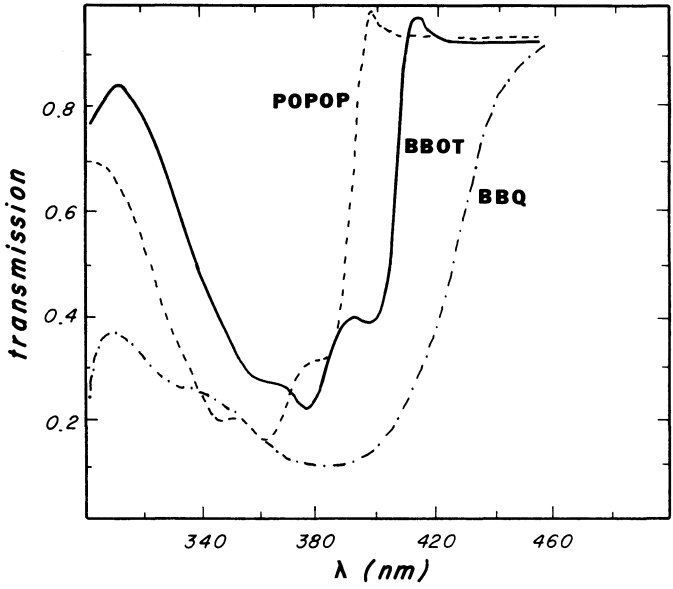
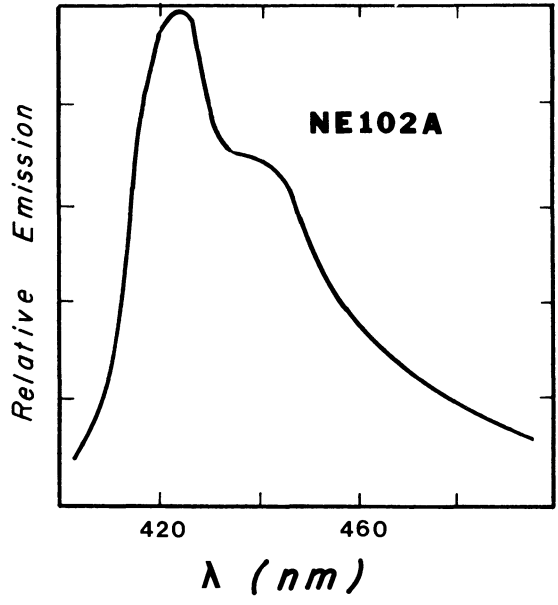


Figure 7.4 Emission spectrum of NE102A plastic scintillator. (Adapted with permission of Thorn EMI Gencom, Inc.)



Downloaded from https://www.cambridge.org/core. UNIVERSIDAD AUTONOMA METROPOLITANA, on 14 Nov 2026 at 11:01:54, subject to the Cambridge Core terms of use, available at https://www.cambridge.org/core/terms. https://doi.org/10.1017/9781009290098.008

which diminishes their light collection efficiency. Any large scintillator is affected by attenuation of the scintillation light traveling through the counter. The distance for the light intensity to fall to $1/e$ of its initial value is called the attenuation length and is typically on the order of 1 m.

Plastic scintillator may also be obtained in the form of thin (1–4-mm-diameter) optical fibers. Such scintillators may prove useful for a fine-grained hodoscope in a high rate environment. The scintillator is clad with a thin layer of material with a lower index of refraction than the scintillator. Encouraging results were obtained with scintillator clad with 200 μm of heat-cured silicone [10]. The major problems are in finding a suitable method for readout and in deterioration from handling.

The scintillation process also occurs in pure noble gases [11]. Atoms excited by the energy loss of a passing particle may dissipate $\sim$ 20% of the excitation energy through the emission of ultraviolet light. The emission

Table 7.3. *Properties of common plastic scintillators*

Type	Light[a] output	λ_{max}[b] (nm)	Attenuation[c] length (cm)	Risetime (ns)	Decay[d] time (ns)	Pulse FWHM (ns)
NE 102A	58–70	423	250	0.9	2.2–2.5	2.7–3.2
NE 104	68	406	120	0.6–0.7	1.7–2.0	2.2–2.5
NE 104B	59	406	120	1	3.0	3
NE 110	60	434	400	1.0	2.9–3.3	4.2
NE 111	40–55	375	8	0.13–0.4	1.3–1.7	1.2–1.6
NE 114	42–50	434	350–400	~1.0	4.0	5.3
Pilot B	60–68	408	125	0.7	1.6–1.9	2.4–2.7
Pilot F	64	425	300	0.9	2.1	3.0–3.3
Pilot U	58–67	391	100–140	0.5	1.4–1.5	1.2–1.9
BC 404	68	408	—	0.7	1.8	2.2
BC 408	64	425	—	0.9	2.1	~2.5
BC 420	64	391	—	0.5	1.5	1.3
ND 100	60	434	400	—	3.3	3.3
ND 120	65	423	250	—	2.4	2.7
ND 160	68	408	125	—	1.8	2.7

[a] Percentage of anthracene.
[b] Wavelength of maximum emission.
[c] $1/e$ length.
[d] Main component.
Source: Catalog, Nuclear Enterprises; Catalog, Bicron Corporation; Catalog, National Diagnostics; M. Moszynski and B. Bengtson, Nuc. Instr. Meth. 158: 1, 1979; G. D'Agostini et al., Nucl. Instr. Meth. 185: 49, 1981.

Downloaded from https://www.cambridge.org/core. UNIVERSIDAD AUTONOMA METROPOLITANA, on 14 Nov 2026 at 11:01:54, subject to the Cambridge Core terms of use, available at https://www.cambridge.org/core/terms. https://doi.org/10.1017/9781009290098.008

spectra consist of a sharp peak near the threshold, together with a much broader continuum enhancement. Table 7.4 lists the threshold wavelength of the emission spectra and a rough estimate of the center of the enhanced portion of the spectrum. The continuum portion of the spectrum results from transitions from vibrationally excited states to the ground state. The emission spectrum is practically independent of the type of incident particle but is strongly affected by the gas pressure.

Another class of scintillating material is scintillation glass. Type SCG1-C scintillation glass contains about 43% BaO as a high Z material [12]. A small percentage of Ce_2O_3 added to the glass produces scintillation light directly and absorbs any Cerenkov light in the glass and reemits it at a longer wavelength. It has a radiation length of 4.35 cm and a fluorescent decay time of $\sim$ 70 ns. Scintillation glass may be preferable to lead glass in certain calorimeter applications. It produces about 5 times as much light as SF5 lead glass and has better radiation resistance. The measured energy deposition was linear for 2 – 17-GeV positrons [12]. The energy resolution was $\sigma/E = 1.64\% + 1.13\%/\sqrt{E}$, compared to typical lead glass resolution $\sigma/E \simeq 1\% + 4.5\%/\sqrt{E}$. Scintillation glass can be used in more extreme environmental conditions than other scintillators, although it is sensitive to the presence of ultraviolet radiation.

7.2 Light collection

Once the scintillator light has been produced, it must be efficiently transported to the face of a photomultiplier tube. This is often one of the more difficult aspects of designing a scintillation counter. Photomultipler tubes (PMTs) cannot operate in a high magnetic field, and so it may be necessary to locate the tube a large distance from the scintillator. The scintillator often covers a much larger area than the photocathode

Table 7.4. *Scintillation of pure noble gases*

Gas	Threshold wavelength (nm)	"Center" wavelength (nm)
He	60.0	75
Ne	74.4	82
Ar	106.7	125
Kr	123.6	150
Xe	147.0	172

Source: A. Breskin et al., Nuc. Instr. Meth. 161: 19, 1979; Y. Tanaka, A. Jursa, and F. LeBlanc, J. Opt. Soc. Am. 48: 304, 1958.

Downloaded from https://www.cambridge.org/core. UNIVERSIDAD AUTONOMA METROPOLITANA, on 14 Nov 2026 at 11:01:54, subject to the Cambridge Core terms of use, available at https://www.cambridge.org/core/terms. https://doi.org/10.1017/9781009290098.008

surface of the tube. In some applications it may be required to collect light uniformly over the entire scintillator volume.

Light is directed to the tube by using either a light guide or a fluorescent converter. Light guides are usually constructed from plastic, although for certain applications the light is sometimes propagated through an enclosed volume of air to the PMT. The light travels down the guide via total internal reflection. On the other hand, a fluorescent converter contains a wavelength shifter, which absorbs the incident radiation and reemits it isotropically at longer wavelengths. The light guides collect light more efficiently, but the fluorescent converters are more useful for providing a compact readout in large area applications.

Let us first consider a rectanglular slab of scintillator or wavelength shifter bar. Light will be emitted isotropically from the scintillator. When the emitted light strikes a surface, total internal reflection will occur for incident angles greater than the critical angle θ_c, given by

$$\sin \theta_c = n_0/n \tag{7.3}$$

where n (n_0) is the index of refraction for the medium in (outside of) which the light is traveling. For simplicity, we take the outside medium to be air, so that $\sin \theta_c = 1/n$. The angle θ_c is measured with respect to the normal to the surface. The higher the value of n for the material, the smaller the critical angle, and the greater the range of incident angles that undergo total internal reflection.

The fraction of the emitted light transmitted via total internal reflection in one direction along the slab is

$$\begin{aligned} f &= \frac{1}{4\pi}\int_0^{\theta_c} 2\pi \sin\theta \, d\theta \\ &= \frac{1}{2}\left(1-\frac{1}{n}\sqrt{n^2-1}\right) \end{aligned} \tag{7.4}$$

Note that this result is independent of the slab dimensions. For typical plastic scintillator with $n = 1.58$, Eq. 7.4 gives $f = 0.113$.

An improvement in light transmission in small counters can be achieved by using a reflector on the end of the scintillator opposite to the collection direction. This subject has been studied in detail by Keil [13]. The reflectors may be either specular or diffuse and may be in direct contact with the medium or separated by a small air gap. Reflectors on the other four sides of the slab will in general have a much smaller influence on the collection efficiency.

For specular reflectors, such as aluminum foil, the emitted light fraction collected (neglecting attenuation) is increased to

Downloaded from https://www.cambridge.org/core. UNIVERSIDAD AUTONOMA METROPOLITANA, on 14 Nov 2026 at 11:01:54, subject to the Cambridge Core terms of use, available at https://www.cambridge.org/core/terms. https://doi.org/10.1017/9781009290098.008

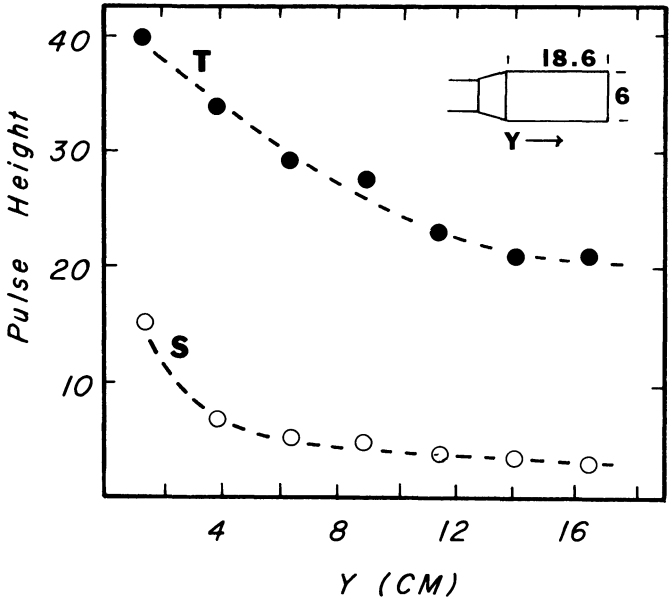
$$f_{\text{spec}}^{\text{air}} = (1+R)f \tag{7.5}$$

where R is the reflectivity. The superscript "air" means that the output face of the scintillator is connected to the next stage of the light collection system via an air gap. This equation holds for both direct and separated coupling to the reflector, although the case with a small reflector gap generally gives better results. If the output edge is coupled to the following stage using an optical contact medium, such as silicon oil, the emitted light fraction is increased. When using a diffuse reflector, such as TiO_2 paint, in direct contact with the scintillating medium, there is no longer any correlation between the directions of the light rays before and after the reflection.

Measurements of the effect of a specular surface on the light collection is shown in Fig. 7.5. The relative pulse height and uniformity of response is much better using total internal reflection than when the reflections take place off a vacuum deposited aluminum surface [14]. An exception to this occurs for the scintillator surface opposite from the PMT.

Plastic counters are loosely wrapped with aluminum foil to capture

Figure 7.5 Relative light collection from a test scintillator using (T) totally reflecting surfaces and (S) vacuum-deposited aluminum surface. The inset shows the test counter dimensions in centimeters. (After D. Crabb, A. Dean, J. McEwen, and R. Ott, Nuc. Instr. Meth. 45: 301, 1966.)



Downloaded from https://www.cambridge.org/core. UNIVERSIDAD AUTONOMA METROPOLITANA, on 14 Nov 2026 at 11:01:54, subject to the Cambridge Core terms of use, available at https://www.cambridge.org/core/terms. https://doi.org/10.1017/9781009290098.008

light that does not undergo total internal reflection and escapes from the surface. The counter is made light tight by wrapping black tape over the foil.

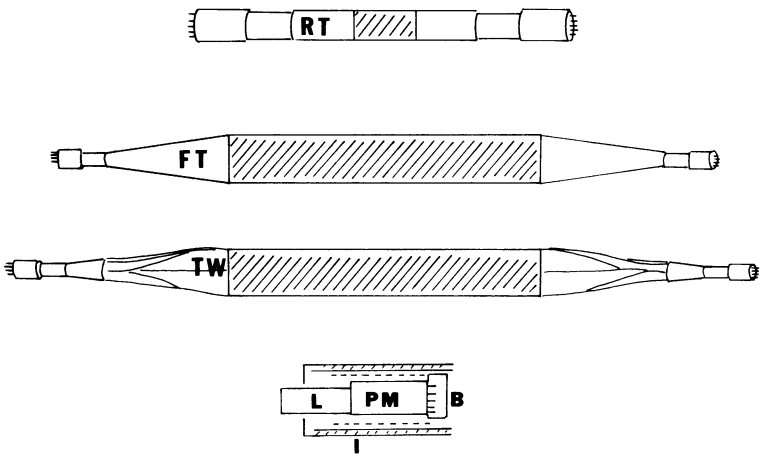
The intensity of light traveling through scintillator or plastic guides roughly follows a relation of the form

$$I(x) = I_{0s}\exp(-x/d_s) + I_{0l}\exp(-x/d_l) \tag{7.6}$$

where the characteristic distances d_s and d_l are properties of the material. The attenuation results from atomic absorption and scattering from surface imperfections, such as scratches or microscopic cracks. Short wavelength light (<360 nm) is strongly absorbed in plastics. This absorption gives rise to the short distance attenuation characterized by d_s. The attenuation of the remaining longer wavelength light is then characterized by d_l.

When the cross section of the scintillator differs significantly from that of the face of the PMT, it is necessary for most light rays to undergo a series of reflections in a light guide before arriving at the tube. The presence of the light guide improves the homogeneity of response of the scintillator [13]. Light guides are typically constructed from acrylic plastics such as lucite. Three light pipe constuctions are illustrated in Fig. 7.6. The rectangular (RT) connection is used for small pieces of scintillator [15]. In the fishtail (FT) arrangement the light pipe is gradually deformed from the

Figure 7.6 Types of light guides: (RT) rectangular, (FT) "fish tail," (TW) two twisted strips. The bottom figure shows a photomultiplier tube assembly (PM) with base (B), standard coupling piece of light guide (L), mu metal shield (dotted lines), and soft iron shield (I). (After G. D'Agostini et al., Nuc. Instr. Meth. 185: 49, 1981.)



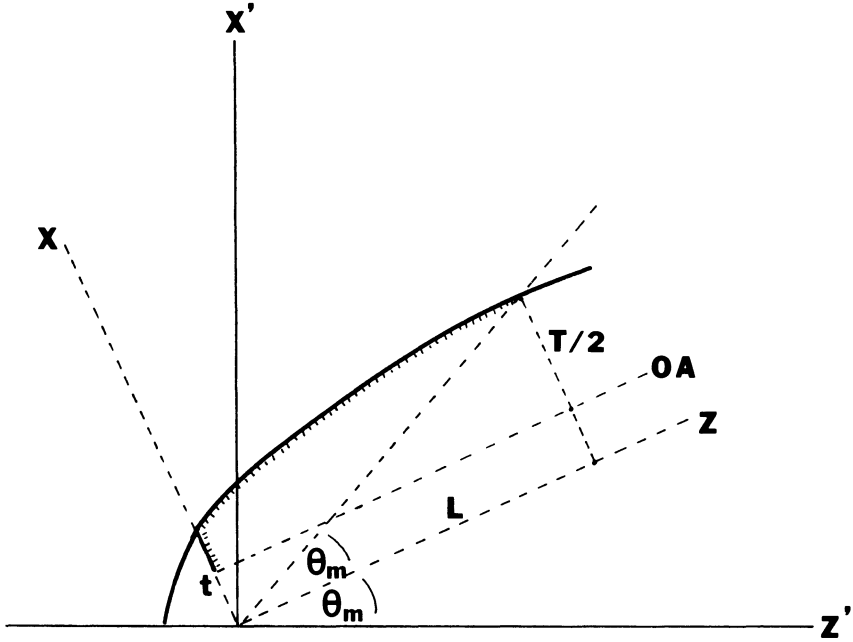
Downloaded from https://www.cambridge.org/core. UNIVERSIDAD AUTONOMA METROPOLITANA, on 14 Nov 2026 at 11:01:54, subject to the Cambridge Core terms of use, available at https://www.cambridge.org/core/terms. https://doi.org/10.1017/9781009290098.008

shape of the scintillator edge to the shape of the photomultiplier window. In the twisted pipe (TW) arrangement the rectangular shape of the scintillator edge is transformed into a square approximately the size of the PMT with a large number of smaller twisted pieces. The twisted arrangement is generally the most efficient.

Liouville's theorem presents a fundamental limitation on the transmission of light through the pipe [16]. The theorem requires that the light flux per unit solid angle not increase while propagating in the pipe. This has the consequence that the maximum fraction of light that can be transmitted is A_{pm}/A_{sc}, where A_{pm} (A_{sc}) is the area of the photomultiplier face (scintillator edge) and $A_{pm} < A_{sc}$.

The light collection efficiency may be improved by using a light collecting cone [17, 18]. Figure 7.7 shows the construction of a Winston cone, which is commonly used before the PMT in Cerenkov counters. The cone is designed to optically focus light at angles up to θ_{max} with respect to the optical axis onto a focus on the PMT face. The surface of the collector is a

Figure 7.7 Geometry of the Winston cone. The face of the PMT lies along t. Half of a section of the cone is shown with hash marks. The 3-dimensional cone is made by revolving the hashed surface around the optical axis $0A$.



Downloaded from https://www.cambridge.org/core. UNIVERSIDAD AUTONOMA METROPOLITANA, on 14 Nov 2026 at 11:01:54, subject to the Cambridge Core terms of use, available at https://www.cambridge.org/core/terms. https://doi.org/10.1017/9781009290098.008

parabola in the primed coordinate system and is given by the equation

$$r(\theta) = \frac{1+\sin\theta_{max}}{1-\cos(\theta+\theta_{max})}t \tag{7.7}$$

where t is the diameter of the PMT and θ_{max} is the maximum accepted angular divergence. The length of the cone is

$$L = \frac{1+\csc\theta_{max}}{2\tan\theta_{max}}t \tag{7.8}$$

while the opening of the collector is

$$T = t/\sin\theta_{max} \tag{7.9}$$

Light guides are usually connected optically to the PMT with grease or cement with an index of refraction greater than that of the light guide, so that there is no total internal reflection from the PMT window.

7.3 Photomultiplier tubes

The great utility of scintillation counters is made possible by photomultiplier tubes (PMT), which convert the scintillator light and amplify it into an electrical pulse suitable for use with decision making, fast electronics. A schematic of a PMT is shown in Fig. 7.8. We shall discuss the characteristics of a typical tube, the RCA 8575. Properties of this and some other commercially available photomultiplier tubes are given in Table 7.5.

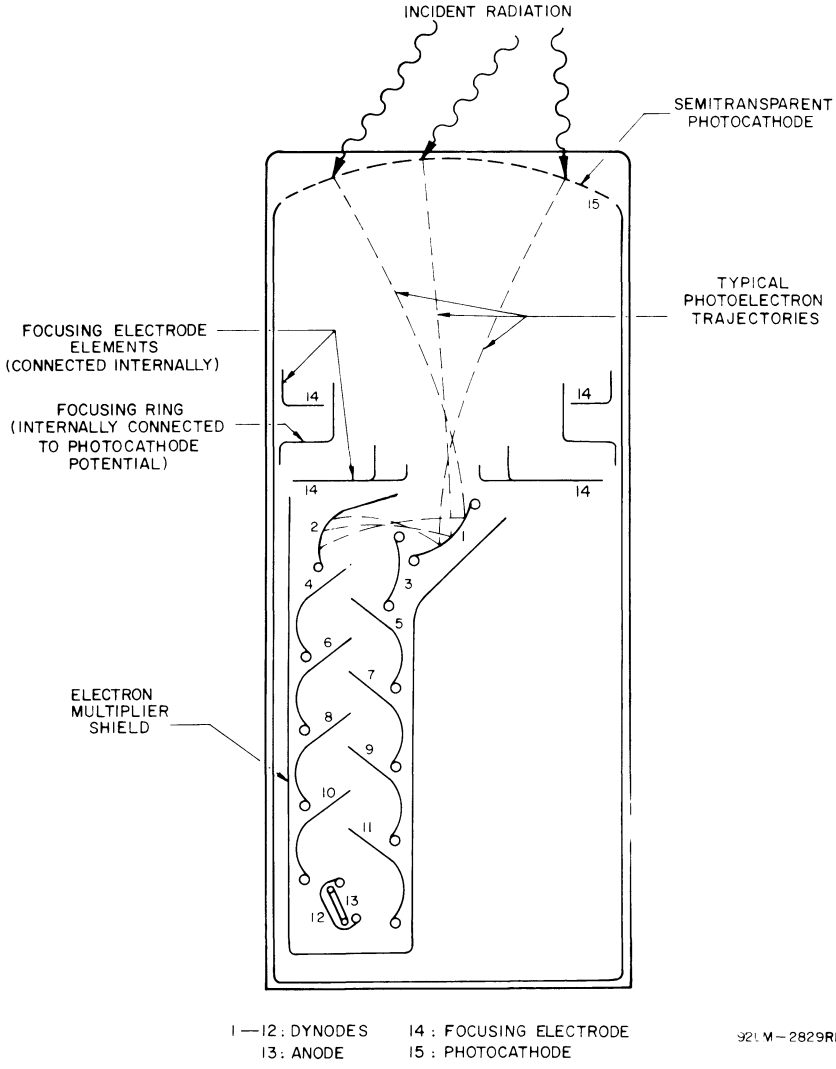
The incident light from the scintillator or light guide falls upon a semi-transparent photocathode. The surface is coated with a material that has a low work function in order to facilitate the emission of electrons from the photocathode by the photoelectric effect. A bialkalai material such as K-Cs-Sb is commonly used. The number of emitted electrons per incident photon, or quantum efficiency, is shown in Fig. 7.9. The quantum efficiency for this tube peaks in the near ultraviolet part of the spectrum and falls off in the visible region. Figure 7.9 also shows the absolute responsivity S (or radiant sensitivity) of the photocathode. This expresses the photoelectric current in terms of the incident radiant power. The two quantities are related by the expression QE (%) = $123.95S$ (mA/W)/λ(nm). The number of photons reaching the photocathode surface also depends on the type of window material used in the tube. Fused silica can extend the accepted wavelength interval several hundred nanometers below that of normal borosilicate glass.

The emitted photoelectrons are accelerated and focused onto the first dynode of the tube. The tube has a number of dynodes made of materials

Downloaded from https://www.cambridge.org/core. UNIVERSIDAD AUTONOMA METROPOLITANA, on 14 Nov 2026 at 11:01:54, subject to the Cambridge Core terms of use, available at https://www.cambridge.org/core/terms. https://doi.org/10.1017/9781009290098.008

with large secondary emission (e.g., Cu-Be or BeO). Typically four electrons may be emitted for each incident electron. The multiplication continues for many stages before the current is collected at the anode. The overall amplification of a 12-stage tube is then several 10^7. The exact amplification depends critically on the high voltage applied between the dynodes. The RCA 8575 pulse has a typical risetime of 3 ns and a transit time of 40 ns with 1800 V between the anode and the cathode.

Figure 7.8 Schematic diagram of the RCA 8575 photomultiplier tube. (Courtesy of RCA, New Products Division, Lancaster, PA.)



Downloaded from https://www.cambridge.org/core. UNIVERSIDAD AUTONOMA METROPOLITANA, on 14 Nov 2026 at 11:01:54, subject to the Cambridge Core terms of use, available at https://www.cambridge.org/core/terms. https://doi.org/10.1017/9781009290098.008

Downloaded from https://www.cambridge.org/core. UNIVERSIDAD AUTONOMA METROPOLITANA, on 14 Nov 2026 at 11:01:54, subject to the Cambridge Core terms of use, available at https://www.cambridge.org/core/terms. https://doi.org/10.1017/9781009290098.008

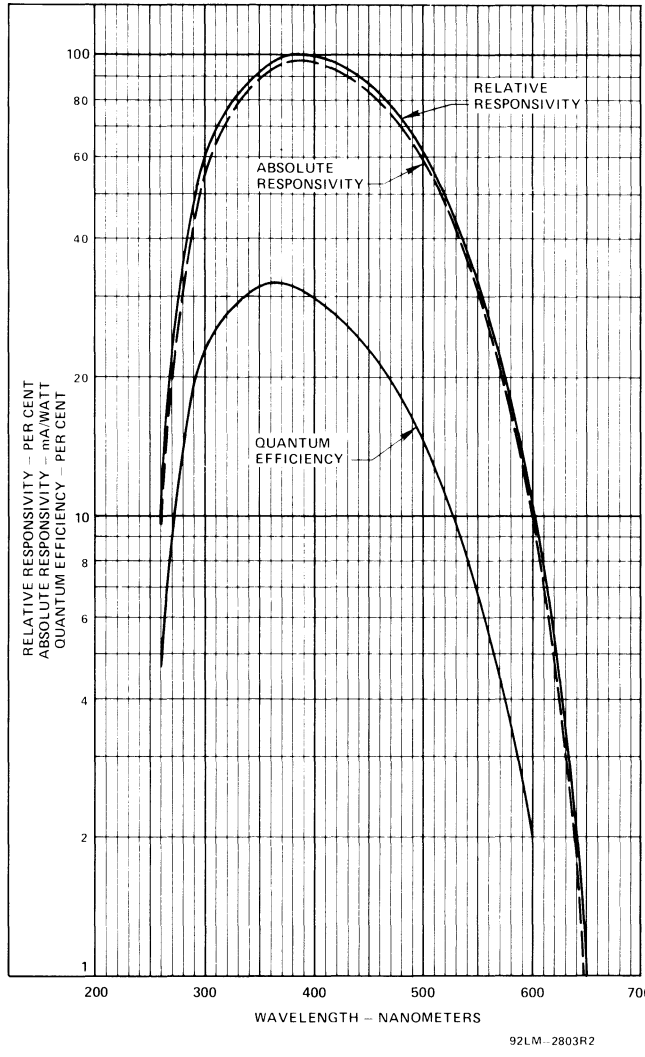
Table 7.5. *Some common photomultiplier tubes*

		Useful diameter (mm)	Gain ($\times 10^6$)	λ, peak response (nm)	Quantum efficiency at peak (%)	Risetime (ns)
EMI	9807B	46	6.7	390	27	2
	9826B	13	3.3	350	20	2.2
	9829B	46	6.7	390	29	2
	9839B	45	6.7	390	27	3
Hammamatsu	R647-01	10	1	420	25	2.3
	R1449	460	10	420	22	18
	R1635	8	1	420	24	0.8
RCA	8575	46	14	385	31	2.5
	8850	46	14	385	31	2.5
	8854	114	40	400	27	3
	C31024	46	5	400	30	1.5
Phillips (Amperex)	XP 2020	44	30	400	26	1.5
	XP 2041	110	30	400	26	2.0
	XP 2230	44	30	400	26	1.6
	56AVP	44		437	17	2.1

Source: Thorn EMI Gencom, Inc., Plainview, NY; Hammamatsu Corp., Middlesex, NJ; RCA, Electro-optics, Lancaster, PA; Amperex Electronics Corp., Hicksville, NY.

Some relevant consideration of tube performance include the photocathode size, the spectral sensitivity, uniformity of response over the photocathode surface, and pulse spread for different electron trajectories. Some tubes are specially designed to have greater response in the ultraviolet region and may use quartz entrance windows. Two other important effects are afterpulsing and dark current. Afterpulsing arises when an ion from the residual gas in the tube or from one of the dynodes makes it back

Figure 7.9 Spectral response characteristics of the RCA 8575 photomultiplier tube. (Courtesy of RCA, New Products Division, Lancaster, PA.)



Downloaded from https://www.cambridge.org/core. UNIVERSIDAD AUTONOMA METROPOLITANA, on 14 Nov 2026 at 11:01:54, subject to the Cambridge Core terms of use, available at https://www.cambridge.org/core/terms. https://doi.org/10.1017/9781009290098.008

to the photocathode and initiates a second pulse. Dark current is the current in the tube when no input light is present. This arises chiefly from the thermal emission of electrons from the photocathode. Other sources include induced radioactivity, scintillation, and Cerenkov processes in the glass envelope of irradiated tubes [19] and potential differences between the glass envelope and photocathode. An electrostatic shield or mylar insulation is sometimes used to prevent current from flowing through the glass.

The high voltage distribution system is basically a resistor divider network. A typical circuit is shown in Fig. 7.10. Capacitances are used with the last dynodes to help maintain the high voltages. The current flowing through the divider to each dynode is the source of the additional electrons that enter the PMT pulse. Limitations on this current can cause the linearity of the tube to decrease for high incident light fluxes. In this case not enough current is available, and the amplification drops off. This effect can be reduced by connecting special high current sources to the last dynode stages. The high voltage supply must be very stable if the tube amplification is to remain constant. The high voltage setting may be determined with the aid of a small radioactive source by looking at the output pulses from the tube on a scope or pulse height analyzer. Often small "button" sources are wrapped inside the counter next to the scintillator. This allows convenient checking of the tube's gain.

PMTs should not be operated in a high helium environment since the gas can permeate the tube. When used continuously at a high current, the tube fatigues and loses amplification. The gain can usually be restored after a quiescent period.

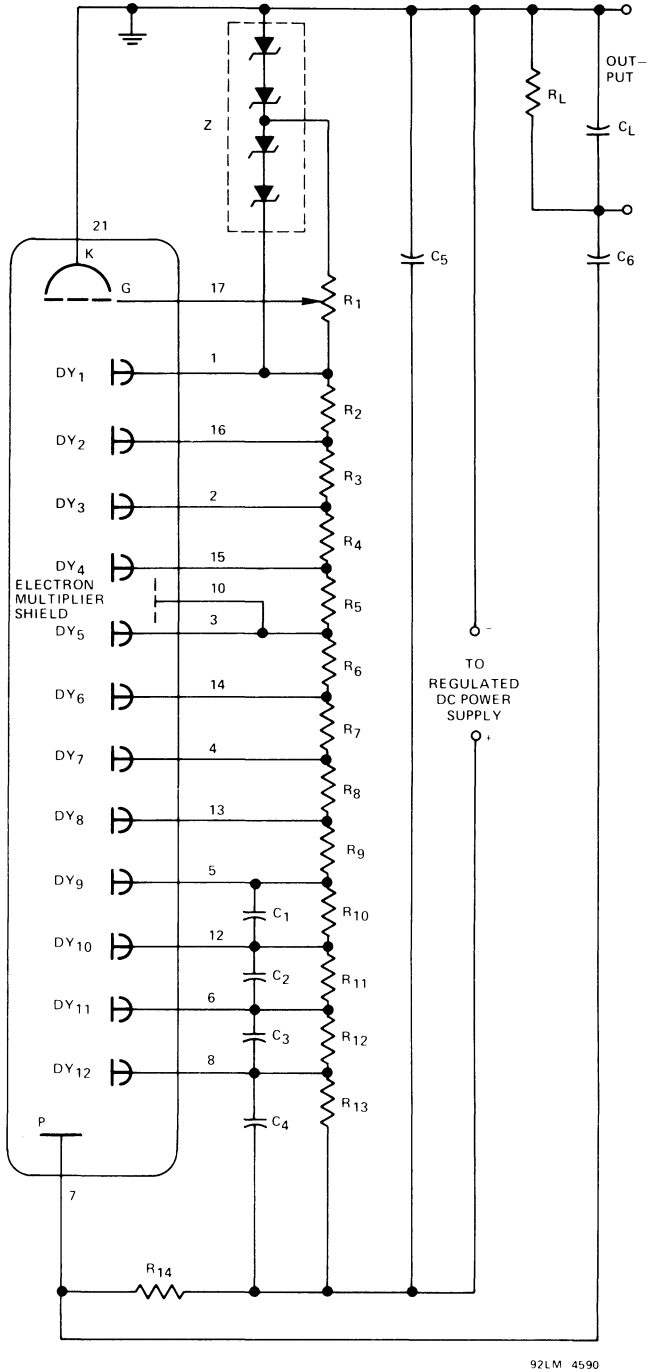
Photomultiplier tubes are very sensitive to the presence of magnetic fields, which upset the delicate focusing conditions in the tube. For this reason, the tube is usually surrounded by a high permeability "mu metal" shield. Magnetic flux lines in the vicinity of the tube tend to be funneled into the shield. The shielding effect is enhanced by leaving a small gap between the tube and the shield. The shield should extend at least one shield diameter beyond the photocathode. For very strong magnetic fields multiple layers of shielding may be necessary. The outermost shield should be made of soft iron, which has a large saturation induction [19].

7.4 Performance

The most common use of scintillation counters is for triggering. The signals from the scintillators can be used by the fast electronics to decide whether to activate other apparatus, such as drift chambers, and whether to record the information from the event. Because of random

Downloaded from https://www.cambridge.org/core. UNIVERSIDAD AUTONOMA METROPOLITANA, on 14 Nov 2026 at 11:01:54, subject to the Cambridge Core terms of use, available at https://www.cambridge.org/core/terms. https://doi.org/10.1017/9781009290098.008

Figure 7.10 Typical photomultiplier tube base circuit. (Courtesy of RCA, New Products Division, Lancaster, PA.)



Downloaded from https://www.cambridge.org/core. UNIVERSIDAD AUTONOMA METROPOLITANA, on 14 Nov 2026 at 11:01:54, subject to the Cambridge Core terms of use, available at https://www.cambridge.org/core/terms. https://doi.org/10.1017/9781009290098.008

tube noise, the signal from the scintillation counter is required to arrive in coincidence with the signal from another element. Sometimes a scintillator signal may be required in anticoincidence with another signal. This is the case, for example, with a hole counter in a beamline, where we wish to eliminate particles in the beam halo. Anticounters could also be used around the target region when we wish to ensure the production of neutral particles.

A scintillator can be used to measure the differential energy loss dE/dx of particles. For small momenta the light output is proportional to the deposited energy. Gamma ray energies can be efficiently measured in NaI crystal scintillators. The high Z facilitates conversion into electron pairs that shower in the crystal. Liquid scintillators are commonly used as neutron detectors. The neutron interacts in the material, and charged particles that are produced initiate the scintillator light.

Important properties of scintillation counters include the efficiency, energy resolution, spatial resolution, and time resolution. We will discuss the first three items in this section and timing in the following section. The efficiency of a counter is ultimately determined by the number of photoelectrons emitted from the photocathode of the PMT. As an example, assume that we have a 1-cm-thick plastic scintillation counter. A minimum ionizing particle loses approximately 1.7 MeV/cm due to ionization while traversing the scintillator. Typically one photon of scintillation light will be emitted per 100 eV of deposited energy. This corresponds to a conversion of $\sim 2\%$ of the ionization energy to scintillation light. Thus, 17,000 photons should be emitted in the scintillator.

A number of losses prevent all of these photons from being detected by the phototube. Some of the light is attenuated in the scintillator and light guide. For example, NE-102 has an attenuation length of 250 cm. Much of the light strikes the edges at less than the critical angle and escapes, although some of this light is returned after reflection from the aluminum foil wrapping. Assuming a 10% light collection efficiency gives 1700 photons in our example, and assuming a quantum efficiency $\sim 25\%$ for the tube, about 400 of the photons will produce photoelectrons.

Rough design values

Energy loss in plastic = 2 MeV/cm

Scintillation efficiency = 1 photon/100 eV

Collection efficiency = 0.10 (large counter)

Quantum efficiency = 0.25

Downloaded from https://www.cambridge.org/core. UNIVERSIDAD AUTONOMA METROPOLITANA, on 14 Nov 2026 at 11:01:54, subject to the Cambridge Core terms of use, available at https://www.cambridge.org/core/terms. https://doi.org/10.1017/9781009290098.008

In the preceding example we calculated the expected or mean number of photoelectrons. The actual number will follow a Poisson probability distribution. The probability that no photoelectron is emitted is

$$\Pr(0) = e^{-\bar{n}} \tag{7.10}$$

In our example this is $e^{-400} \ll 1$ so that the counter is practically 100% efficient. Conversely, if we have measured the efficiency ϵ of a counter, we can make a crude estimate of the number of emitted photoelectrons from the relation

$$1 - \epsilon = e^{-\bar{n}}$$

so that

$$\bar{n} = -\ln(1 - \epsilon) \tag{7.11}$$

Now let us consider several examples of the performance of actual counters. Mount et al. [20] constructed a set of highly efficient scintillation counters for use as veto counters at the CERN SPS. The inefficiency was made smaller than 10^{-6} by designing counters that could provide at least 14 photoelectrons per particle and by using burst guard discriminators. The amount of accidental vetoing was minimized by shortening the photomultiplier pulse with a resistive clip.

The energy resolution of a scintillation counter is usually determined by sampling the output pulses of the counter with a pulse height analyzer. The energy resolution $\Delta E/E$ is defined as

$$\Delta E/E \simeq \Delta M/\overline{M} \simeq (\bar{n})^{-1/2} \tag{7.12}$$

where $\overline{M}$ is the channel number of the signal peak and ΔM is the FWHM of the peak. The second equality follows from the assumption of Poisson statistics.

Scintillation counters have poor spatial resolution compared with other detectors, such as proportional or drift chambers. The best spatial resolution with scintillation counters occurs when many narrow counters are used in parallel. Such an arrangement is referred to as a scintillation hodoscope. Aubert et al. [21] have constructed a fine grained hodoscope for use in a beam at the CERN SPS. Each plane consisted of sixty 2-mm-wide counters. The spacing was chosen to match the resolution of the experimental apparatus in determining the vertex position. The length of each counter was determined by the beam size. The thickness of the counters was chosen to be 4 mm, so that the efficiency of the counter would exceed 99%. The counters were placed in two slightly overlapping planes to eliminate dead spaces due to the counter wrapping.

Long counters often use a PMT on each end. In this case measurements

Downloaded from https://www.cambridge.org/core. UNIVERSIDAD AUTONOMA METROPOLITANA, on 14 Nov 2026 at 11:01:54, subject to the Cambridge Core terms of use, available at https://www.cambridge.org/core/terms. https://doi.org/10.1017/9781009290098.008

of the pulse height at the bottom (B) and top (T) can be used to estimate the position of the particle trajectory along the counter and in some cases the particle energy. Because of the exponential attenuation of the light traveling from the source to the ends, the position of the source above the counter midplane is

$$y \propto \ln(T/B) \tag{7.13}$$

In the region of relativistic rise, where $dE/dx \propto E$, we have

$$E \propto (BT)^{1/2} \tag{7.14}$$

Measurements of these quantities shown in Fig. 7.11 agree nicely with expectations.

As systems of scintillator hodoscopes or calorimeters become larger and larger, there are increasing problems with monitoring the pulse height and relative timing of each counter. These signals may drift or fail entirely over a period of time. For this reason, many large experiments have developed monitoring systems using LED pulsers or lasers that periodically test the response of all the counters to a known input pulse. Berglund et al. [22] have constructed a laser calibration system for use at CERN. They used an N_2 laser that produced $\sim 10^{14}$ photons in a 3-ns pulse. The light was directed into a bundle of one hundred and sixty 20-m-long optical fibers. The large number of produced photons is necessary because the solid angle for entering a given fiber is very small. The pulse to pulse light variation entering the fiber was $\pm 10\%$. The fibers were first cut to equal lengths and the delays measured. They were then cut a second time according to the measured delays. The final output of the fibers had a 150-ps (rms) time spread and 19% (rms) amplitude variation.

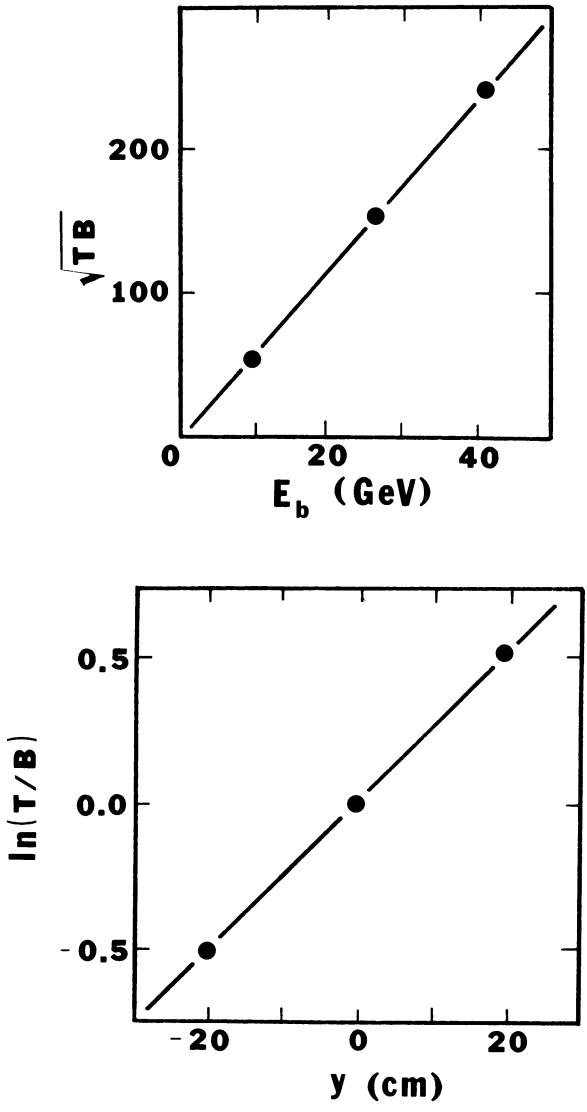
7.5 Timing applications

One of the important applications of scintillation counters is the measurement of time intervals at the nanosecond level. The resolution of a time interval measurement may be determined using the simple apparatus shown in Fig. 7.12. Two small counters S1 and S2 are used for triggering the system. Coincidences between S1 and S2 are used as a gate for an ADC and as a start signal for a TDC. The counter S3, which is being measured, is placed between S1 and S2. The anode pulse from the PMT is discriminated and used to stop the TDC. The dynode signal is linearly inverted and then sent to an ADC. The measured pulse height can be used to correct the TDC for slewing. The FWHM of the resulting spectrum of time intervals is a measure of the time resolution of the system.

Two groups of effects are mainly responsible for the time spread in

Downloaded from https://www.cambridge.org/core. UNIVERSIDAD AUTONOMA METROPOLITANA, on 14 Nov 2026 at 11:01:54, subject to the Cambridge Core terms of use, available at https://www.cambridge.org/core/terms. https://doi.org/10.1017/9781009290098.008

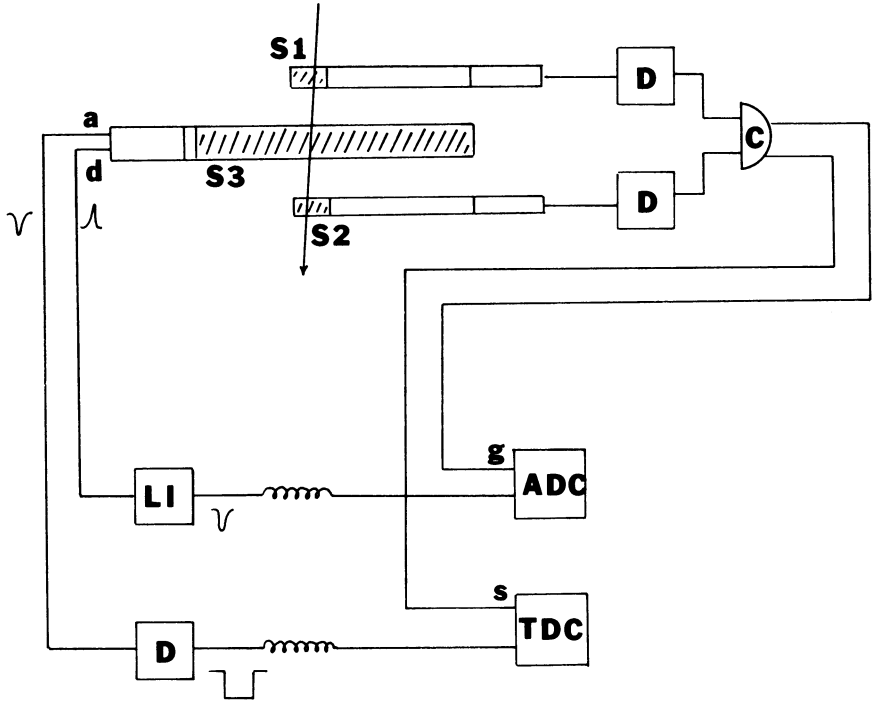
Figure 7.11 Position and energy information derived from a scintillator with tubes at the bottom (B) and top (T). (After C. Bromberg et al., Nuc. Phys. B 171: 1, 1980.)



Downloaded from https://www.cambridge.org/core. UNIVERSIDAD AUTONOMA METROPOLITANA, on 14 Nov 2026 at 11:01:54, subject to the Cambridge Core terms of use, available at https://www.cambridge.org/core/terms. https://doi.org/10.1017/9781009290098.008

scintillation counter signals [23, 24]. The first group of limitations are concerned with variations in the time at which the detector responds to the radiation. Effects due to the scintillator include time variations in the energy transfer from the radiation to the optical levels of the scintillator and the finite decay time of the light emitting state. There are variations in transit time through the light collector. The resolution should be improved if only the light emitted straight to the PMT is utilized. This corresponds to the first part of the light pulse. This effect is one of the main reasons that small counters have significantly better time resolution (~ 50 ps) than do large ones (~ 250 ps). Effects due to the PMT include variations in the transit time from the photocathode to the first dynode due to the spread in initial photoelectron velocities and the location of the photoelectron emission on the photocathode and variations in electron amplification in the tube.

Figure 7.12 A simple arrangement for timing resolution measurements. (S1 – S3) scintillation counters, (D) discriminator, (C) coincidence unit, (LI) linear inverter, (a) anode signal, (d) dynode signal, (g) ADC gate, (s) TDC start.



Downloaded from https://www.cambridge.org/core. UNIVERSIDAD AUTONOMA METROPOLITANA, on 14 Nov 2026 at 11:01:54, subject to the Cambridge Core terms of use, available at https://www.cambridge.org/core/terms. https://doi.org/10.1017/9781009290098.008

The photomultiplier transit time spread can be minimized by increasing the voltage between the photocathode and first dynode. A significant improvement in the time resolution of some tubes can also be obtained by taking the output pulse from an intermediate dynode stage instead of the anode [7]. This apparently results from the fact that electrons traveling from the next to last to the last dynode induce a signal on the anode of some tubes. The anode signal then consists of the directly collected charge plus the induced signal, resulting in a broadened pulse.

The second group of limitations are due to the electronics circuits used to process the PMT pulse. Some form of discriminator must be used to pick off a time from the pulse. The manner in which this is done can make a significant contribution to the timing resolution. Additional contributions come from electronic drift and thermal variations of the signal cable propagation velocity.

An important application of scintillation counters that makes use of their excellent timing capabilities is in time of flight (TOF) systems. This technique has been used for low momentum particles to help extract a signal from the background. For example, the TOF of the recoil proton in elastic scattering is correlated with its kinetic energy [25]. A scatter plot of the two quantities reveals a heavy band due to the protons over a scattered background due to accidentals. A cut around this band can be used to help purify the elastic scattering data sample.

A second and more common use of the TOF technique is to identify particle masses [26]. Imagine two scintillation counters separated by a distance L. A relativistic particle with momentum p will traverse the distance between the counters at a rate ($c=1$)

$$t/L = (3333/p)(p^2+m^2)^{1/2} \qquad \text{ps/m} \tag{7.15}$$

There will be a TOF difference for two equal momentum particles that have different masses. The time difference per flight path L is given by

$$(t_1-t_2)/L \simeq 1667(m_1^2-m_2^2)/p^2 \qquad \text{ps/m} \tag{7.16}$$

Figure 7.13 shows the time separation per meter between p and K, p and π, and K and π as a function of momentum. We note first of all that the time difference is very small. Even with a long 10-m flight path, the time difference between a 1-GeV/c pion and kaon is only 3.8 ns. The other important feature is that the time separation decreases like the square of the momentum. This limits the usefulness of this means of particle identification to momenta below ~ 4 GeV/c. Nevertheless, a large fraction of charged particles are produced with low momentum, even at the high

Downloaded from https://www.cambridge.org/core. UNIVERSIDAD AUTONOMA METROPOLITANA, on 14 Nov 2026 at 11:01:54, subject to the Cambridge Core terms of use, available at https://www.cambridge.org/core/terms. https://doi.org/10.1017/9781009290098.008

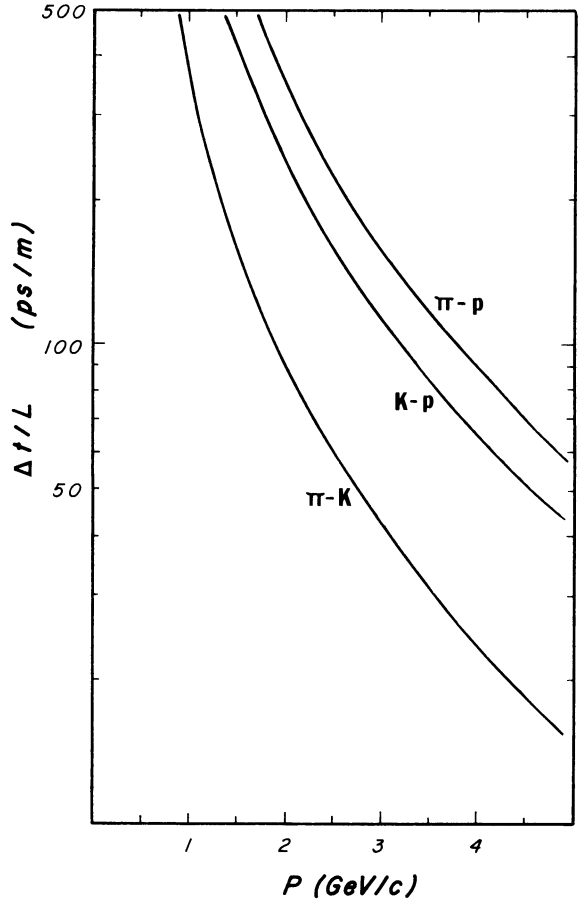
energy accelerators. This method of particle identification is limited by the maximum permissible flight path, the timing resolution, and by systematic errors for large systems of counters.

A measured TOF spectrum for 1.4-GeV/c π and K is shown in Fig. 7.14. The arrival time of a scintillator signal is found to be related to its pulse height by [26]

$$\tau = t - K[(a_0)^{-1/2} - (a)^{-1/2}] - x/v \tag{7.17}$$

where τ is the corrected time, t is the measured time, a is the pulse height, a_0 is a reference pulse height, x/v is a position correction due to the finite

Figure 7.13 The time difference per unit flight path for πK, Kp, and πp as a function of momentum.



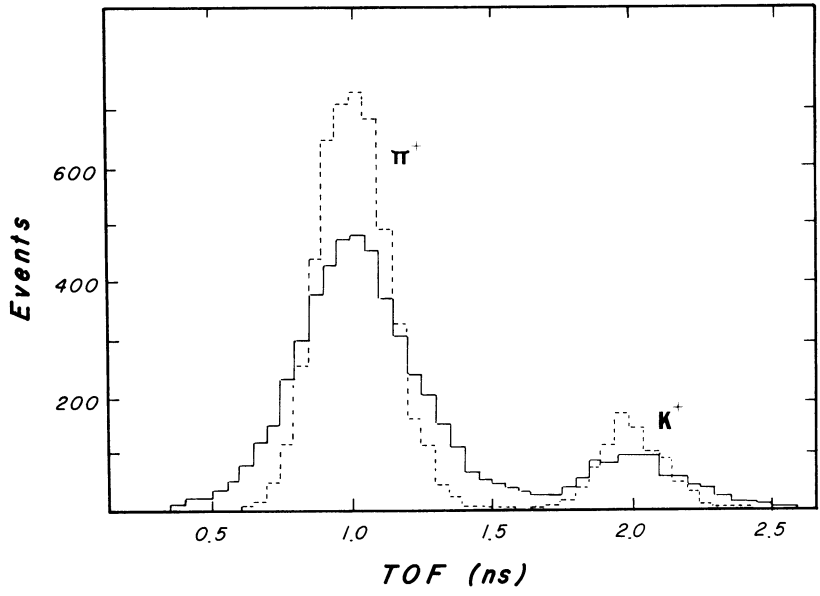
Downloaded from https://www.cambridge.org/core. UNIVERSIDAD AUTONOMA METROPOLITANA, on 14 Nov 2026 at 11:01:54, subject to the Cambridge Core terms of use, available at https://www.cambridge.org/core/terms. https://doi.org/10.1017/9781009290098.008

time required for light to travel a distance x with effective velocity v, and K is a free parameter. Note in Fig. 7.14 how the TOF distribution is sharpened with the application of the pulse height correction.

In timing applications attention must be paid to the risetime and FWHM of the light pulses created in the scintillator. Special scintillators such as NE-111 have been formulated especially for fast timing purposes. PMTs should be chosen to have as small a time jitter as possible. It has also been found that it is beneficial not to cover the entire counter with aluminum foil [15]. This reduces the overall efficiency, but the loss comes at the expense of slow photons, which make the pulse height correction less precise. The time resolution is found to be proportional to $(L/N_e)^{1/2}$, where L is the length of the counter and N_e is the mean number of expected photoelectrons [26].

It is fairly common for TOF systems to be incorporated in particle spectrometers. For example, the TASSO spectrometer at PETRA contains a large TOF array for low momentum particle identification [27]. There are a total of 96 separate 1.6-m-high by 33-cm-wide NE-110 scintillation counters. The start time originates from electrostatic pickups inside the beampipe, which signal a beam–beam crossing. Each counter

Figure 7.14 Time of flight spectra for 1.4-GeV/c π and K. Solid lines: raw data. Dashed lines: data corrected for signal pulse height. (After G. D'Agostini et al., Nuc. Instr. Meth. 185: 49, 1981.)



Downloaded from https://www.cambridge.org/core. UNIVERSIDAD AUTONOMA METROPOLITANA, on 14 Nov 2026 at 11:01:54, subject to the Cambridge Core terms of use, available at https://www.cambridge.org/core/terms. https://doi.org/10.1017/9781009290098.008

is viewed from both ends by EMI 9807B PMTs. The signal from each tube is fed into an ADC and a TDC. System operation is monitored using LED and spark gap, optical fiber arrangements. The flight path from the interaction point to the counters was 5.7 m. However, at a point approximately one-third of the way along this path, the particles had to pass through the coils of the TASSO magnet. The resolution of the system was ~450 ps, including a large contribution due to the multiple scattering of the particles passing through the magnet coil.

The MARK III detector at SPEAR used a 48-counter TOF system for particle identification up to 1.2 GeV/c particle momentum [28]. Each individual counter was 5 cm thick, 15.6 cm wide, and 318 cm long. The counters used Pilot F scintillator with XP2020 PMTs at both ends. The counters were mounted on the outer skin of the central drift chambers with a 1-cm styrofoam separator and were located in a 4-kG magnetic field. The perpendicular distance of the counters from the beamline was ~1.1 m. The light guides passed through holes in the iron end yoke. The system was monitored using an N_2 laser–optical fiber system. After all corrections were applied, the system achieved a time resolution of 170–190 ps, depending on the type of particle reaction.

References

[1] J. Birks, *The Theory and Practice of Scintillation Counting,* New York: Macmillan, 1964.
[2] E. Schram, *Organic Scintillation Detectors,* New York: Elsevier, 1963.
[3] R. Heath, R. Hofstadter, and E. Hughes, Inorganic scintillators: A review of techniques and applications, Nuc. Instr. Meth. 162: 431–76, 1979.
[4] A. Melissinos, *Experiments in Modern Physics,* New York: Academic, 1966.
[5] P. Pavlopoulos, M. Hasinoff, J. Repond, L. Tauscher, D. Troster, M. Rousseau, K. Fransson, T. Alberis, and K. Zioutas, The response of a 5 cm ×20 cm BGO crystal to electrons in the 150 to 700 MeV range, Nuc. Instr. Meth. 197: 331–4, 1982; an exhaustive study of BGO can be found in C. Holmes (ed.), International workshop on bismuth germanate, Princeton University report, 1982.
[6] F. Brooks, Development of organic scintillators, Nuc. Instr. Meth. 162: 477–505, 1979.
[7] B. Bengtson and M. Moszynski, Timing improved by the use of dynode signals studied with different scintillators and photomultipliers, Nuc. Instr. Meth. 204: 129–40, 1982.
[8] V. Eckardt, R. Kalbach, A. Manz, K. Pretzl, N. Schmitz, and D. Vranic, A novel light collection system for segmented scintillation counter calorimeters, Nuc. Instr. Meth. 155: 389–98, 1978.
[9] F. Klawonn, K. Kleinknecht, and D. Pollmann, A new type of acrylic scintillator, Nuc. Instr. Meth. 195: 483–9, 1982.
[10] S. Borenstein, R. Palmer, and R. Strand, Optical fibers and avalanche photodiodes for scintillation counters, Physica Scripta 23: 550–5, 1981.
[11] A. Policarpo, Light production and gaseous detectors, Physica Scripta 23: 539–49, 1981.

Downloaded from https://www.cambridge.org/core. UNIVERSIDAD AUTONOMA METROPOLITANA, on 14 Nov 2026 at 11:01:54, subject to the Cambridge Core terms of use, available at https://www.cambridge.org/core/terms. https://doi.org/10.1017/9781009290098.008

[12] B. Cox, G. Hale, P. Mazur, R. Wagner, D. Wagoner, H. Areti, S. Conetti, P. Lebrun, T. Ryan, J. Brau, and R. Gearhart, A measurement of the response of an SCG1-C scintillation glass shower detector to 2–17.5 GeV positrons, Nuc. Instr. Meth. 219: 487–90, 1984.
[13] G. Keil, Design principles of fluorescence radiation converters, Nuc. Instr. Meth. 89: 111–23, 1970.
[14] D. Crabb, A. Dean, J. McEwen, and R. Ott, Optimum design of thin, large area scintillation counters, Nuc. Instr. Meth. 45: 301–8, 1966.
[15] G. D'Agostini, G. Marini, G. Martellotti, F. Massa, A. Rambaldi, and A. Sciubba, High resolution time of flight measurements in small and large scintillation counters, Nuc. Instr. Meth. 185: 49–65, 1981.
[16] R. Garwin, The design of liquid scintillation cells, Rev. Sci. Instr. 23: 755–7, 1952.
[17] H. Hinterberger and R. Winston, Efficient light coupler for threshold Cerenkov counters, Rev. Sci. Instr. 37: 1094–5, 1966.
[18] W. Welford and R. Winston, *The Optics of Non-Imaging Concentrators,* New York: Academic, 1978.
[19] D. Ritson, Scintillation and Cerenkov Counters, in D. Ritson (ed.), *Techniques of High Energy Physics,* New York: Interscience, 1961, Chap. 7.
[20] R. Mount, P. Cavaglia, W. Stockhausen, and H. Wahlen, Highly efficient scintillation counters, Nuc. Instr. Meth. 160: 23–7, 1979.
[21] J. Aubert, G. Bassompierre, G. Coignet, J. Crespo, Y. Declais, L. Massonnet, M. Moynot, P. Payre, C. Peroni, J. Thenard, and M. Schneegans, A high resolution beam hodoscope counter for use in very intense beams, Nuc. Instr. Meth. 159: 47–51, 1979.
[22] S. Berglund, P. Carlson, and J. Jacobson, A laser based time and amplitude calibration system for a scintillation counter hodoscope, Nuc. Instr. Meth. 190: 503–9, 1981.
[23] M. Moszynski and B. Bengtson, Status of timing with plastic scintillation detectors, Nuc. Instr. Meth. 158: 1–31, 1979.
[24] P. Carlson, Prospects of scintillator time of flight systems, Physica Scripta 23: 393–6, 1981.
[25] R. Cool, K. Goulianos, S. Segler, G. Snow, H. Sticker, and S. White, Elastic scattering of $p^{\pm}$, $\pi^{\pm}$, and $K^{\pm}$ on protons at high energies and small momentum transfer, Phys. Rev. D 24: 2821–8, 1981.
[26] W. Atwood, Time of flight measurements, SLAC-PUB-2620, 1980.
[27] K. Bell, J. Blissett, B. Foster, J. Hart, A. Parham, B. Payne, J. Proudfoot, D. Saxon, and P. Woodworth, A large scintillator array for particle identification by time of flight, Nuc. Instr. Meth. 179: 27–38, 1981.
[28] J. Brown, T. Burnett, V. Cook, C. Del Papa, A. Duncan, P. Mockett, J. Sleeman, D. Wisinski, and H. Willutzki, The MARK III time of flight system, Nuc. Instr. Meth. 221: 503–22, 1984.

Exercises

1. Find the critical angle for (a) a plastic scintillator–air interface, (b) a lucite–air interface, and (c) a plastic scintillator–lucite interface.

2. Consider a rectangular slab of scintillator. Show that a fraction
$$f_t = [3(n^2 - 1)^{1/2}/n] - 2$$

Downloaded from https://www.cambridge.org/core. UNIVERSIDAD AUTONOMA METROPOLITANA, on 14 Nov 2026 at 11:01:54, subject to the Cambridge Core terms of use, available at https://www.cambridge.org/core/terms. https://doi.org/10.1017/9781009290098.008

of the isotropically emitted light inside the slab is reflected at all surfaces and is trapped inside the slab, provided that the index of refraction $n \geq 1.414$.

3. Estimate the attenuation length of the test scintillator used in Fig. 7.5.
4. Derive Eqs. 7.7, 7.8, and 7.9 for the Winston cone.
5. Find the mean number of collected photoelectrons corresponding to a detection efficiency of 99.9%. What is the probability of observing half this number of photoelectrons?
6. Estimate how many photons are produced in a 1-cm-thick plastic scintillator by (a) 1-GeV/c protons, (b) 100-MeV/c protons, and (c) 10-GeV/c protons.
7. Design a scintillation counter hodoscope for a hadron beamline with 10^6 particles/sec. and maximum extension of 10×10 cm. Specify a commercially available scintillator and photomultiplier. Make a sketch of the light guide.
8. A plastic scintillator of length L has PMTs directly coupled to both sides. If a passing particle produces a normalized pulse height of 100 mV on the left and 60 mV on the right, find the position of the particle along the counter. How is the apparent position of the particle changed if there are light guides of length $L/4$ on each side with attenuation length $\lambda_{LG} = 2\lambda_{SC}$?
9. What is the difference in flight times for 3-GeV muons and electrons over a 20-m path?
10. What path length would be required to identify 1-GeV/c pions from kaons at the 90% confidence level ($\sim 3\,\sigma$) using time of flight if the timing resolution is 250 ps?

Downloaded from https://www.cambridge.org/core. UNIVERSIDAD AUTONOMA METROPOLITANA, on 14 Nov 2026 at 11:01:54, subject to the Cambridge Core terms of use, available at https://www.cambridge.org/core/terms. https://doi.org/10.1017/9781009290098.008